ICAS 2021 SHANG HAI
International Council of the Aeronautical Sciences
32nd Congress of the International Council of the Aeronautical Sciences
September 6-10, 2021 Pudong Shangri-La, Shanghai, China

LARGE-EDDY SIMULATION OF A SWIRLING AVIATION KEROSENE SPRAY FLAME USING 3-COMPONENT SURROGATE FUELS

Kaidi Wan[1,2], Yunzhe Huang[1,2], Zhenxun Gao[1,2], Yong He[3] & Chongwen Jiang[1,2,*]

[1]Aircraft and Propulsion Laboratory, Ningbo Institute of Technology, Beihang University, Ningbo, 315832, China
[2]National Laboratory for Computational Fluid Dynamics, School of Aeronautic Science and Engineering, Beihang University, Beijing, 100191, China
[3]State Key Laboratory of Clean Energy Utilization, Zhejiang University, Hangzhou 310027, China

Abstract

As a high-fidelity simulation technique, large-eddy simulation (LES) is an important numerical approach to investigate the complex phenomena inside the aviation engine combustors including atomization of fuel jets, beak-up of fuel droplets, evaporation, and turbulent mixing of fuel and air. The present paper describes a coupling method of flamelet generated manifold (FGM) chemistry table built with 3-component surrogate kerosene skeletal mechanism and the artificial thickened flame (ATF) model under the LES framework. The complex chemical kinetic effects of kerosene combustion can then be accounted in LES with a minor computational cost. A swirling-stabilized aviation kerosene burner configuration is investigated with the proposed approach and encouraging results are obtained. The interactions between the partially premixed flame and the evaporating droplets are well predicted by the LES simulation.

Keywords: Large-eddy simulation; Turbulent combustion; Kerosene spray; Swirling flame; Surrogate fuel

1. Introduction

With the economic and social development of the world, the capacity of aviation market is rapidly increasing nowadays. On the other hand, due to the more and more strict environmental standards, advanced green combustion engines must be developed for aviation vehicles. The combustion process in aviation engines involve complex phenomena including atomization of fuel jets, beak-up of fuel droplets, evaporation, and turbulent mixing of fuel and air. It can be very expensive to quantitative measure these processes inside real aviation engines. With the rapid growing of computational capability around the world, the high-fidelity numerical simulation methods such as large-eddy simulation (LES) and direct numerical simulation (DNS) appear as effective tools to better understand the complex turbulent combustion processes of aviation fuels in realistic configuration [1], which is urgently required in developing advanced green aviation engines.

Kerosene type fuels are the major fuels of aviation engines, including the commercial jet fuels Jet-A1 and RP-3 (in China), and also the military jet fuel JP-8. Kerosene type fuels are composed of hundreds of aliphatic and aromatic hydrocarbon compounds, while the detailed combustion mechanisms of many of them are unavailable. Hence, the combustion of kerosene fuels cannot be directly described by a detailed chemical mechanism. Practically, surrogate fuels are employed as a useful approach in developing chemical mechanisms for kerosene fuels [2]. Surrogate fuels are mixtures of few hydrocarbon compounds and the concentration of each compound is adjusted to approximate the physical and chemical properties of kerosene type fuels. Two- and three-component surrogates have been found to successfully reproduce the general combustion characteristics of aviation kerosene fuels. The components of these surrogates usually include a long chain aliphatic species and a cyclic compound. The aliphatic species is often n-decane or n-dodecane while the cyclic species can be trimethylbenzene, propylbenzene, methylcyclohexane and many others.

The detailed and skeletal chemical mechanisms of the kerosene surrogates usually contain more

than 50 species and hundreds of elementary reactions. The large size of the mechanisms limits their applications to only low-dimensional canonical combustion problems. It would be too expensive to directly adopt such a large mechanism in three-dimensional (3D) high-fidelity numerical simulations. To account for complex chemical kinetics, flamelet-based combustion models offer a cost-effective way in 3D simulations [3]. Two equivalent flamelet approaches, i.e., flamelet-generated manifold (FGM) and flamelet progress variable (FPV), which are developed from premixed and non-premixed combustion concepts respectively, are both successfully employed for describing the partially premixed combustion process of kerosene surrogate fuels. In these approaches, the complex chemical processes are mapped to a reduced system of several tracking scalars. The species mass fractions and temperature are tabulated against these tracking scalars along with the sources of the scalars. During the 3D numerical simulations, the chemistry table should be loaded into the memory of computers and only the transport equations of the tracking scalars need to be solved. The species mass fractions and temperature can then be obtained by looking up the chemistry table with the values of tracing scalars at each grid point.

In the present study, the spray flame structure of a swirling aviation kerosene jet configuration is investigated via large-eddy simulation. The aviation kerosene fuel is represented using a 3-component surrogate fuel. The FGM chemistry table is built from canonical one-dimensional (1D) premixed flames, to then implemented into the LES solver accounting for the complex chemical kinetics of the turbulent kerosene flame. The performance of the spray flamelet FGM-LES approach is discussed.

2. Swirling kerosene spray flame

The swirling kerosene spray flame was investigated experimentally by Sheen [4]. As shown in Fig. 1, the cylindrical combustor features a length of 500 mm and a diameter of 200 mm. Annular inlet of swirling air is located at 50 mm upstream of the front of the combustor. The liquid kerosene injector with a diameter of 0.25 mm is located at the center of the combustor front plate. Aviation kerosene fuel is injected as fine hollow cone spray into the combustor. The exit of the combustor is open to the atmosphere. The operating parameters of the kerosene spray combustor are summarized in Table 1.

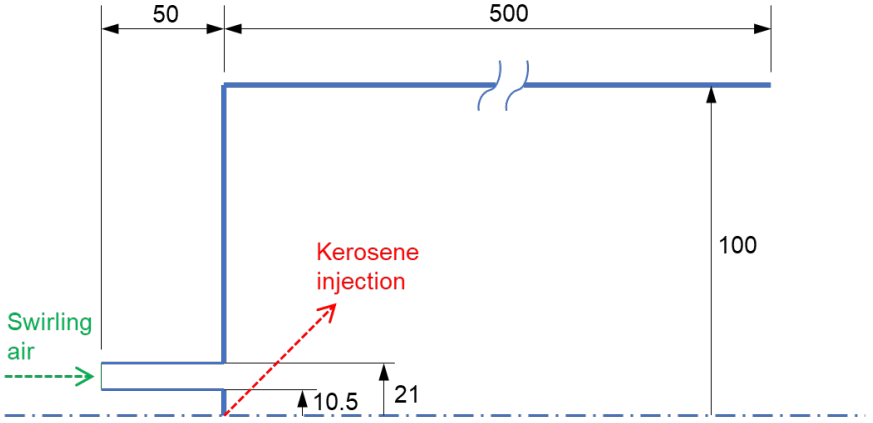

Figure 1 – Schematic illustration of the kerosene combustor.

3. Tabulation of kerosene chemistry

3.1 3-component surrogate fuel

The aviation kerosene fuel is modeled by a 3-component surrogate fuel, which is composed of n-$C_{10}H_{22}$, PhC_3H_7 and cyC_9H_{18}. The detailed compositions and the physical properties of the surrogate fuel are summarized in Table 2 [5].

The combustion of the 3-component surrogate fuel is described by the skeletal LUCHE mechanism, which consists of 91 species and 694 reactions [6]. FGM chemistry tabulation approach is employed to account for the complex chemistry kinetics effects in 3D simulations with an affordable computational cost.

Table 1 – Operating parameters of the combustor

	Swirling air inlet	Liquid kerosene inlet
Temperature (K)	300	300
Mass flow rate (g/s)	26.51	0.951
Air-to-fuel ratio (-)	27.88	–
Swirl number (-)	0.91	–
Spray cone angle (°)	–	74
Rosin-Rammler distribution		
Mean diameter (μm)	–	60
Minimum diameter (μm)	–	1
Maximum diameter (μm)	–	100
Spread parameter (-)	–	3

Table 2 – Compositions and physical properties of the kerosene surrogate fuel

Composition	$Y_{NC10H22}$ = 0.767388
	Y_{PHC3H7} = 0.131402
	$Y_{CYC9H18}$ = 0.101210
Molar Mass (kg mol^{-1})	0.137
Boiling Temperature (K)	445.1
Evaporation latent heat (J kg^{-1})	289010
Heat capacity of the liquid fuel (J kg^{-1} K^{-1})	2003
Density of the liquid fuel (kg m^{-3})	781

3.2 FGM chemistry tabulation

The FGM chemistry tabulation approach maps the complex chemical trajectories of the 3D simulations to a low-dimensional reduced system with only several tracking scalars. These tracking scalars can be viewed as the principle components of the entire chemical system. The mixture fraction Z and the progress variable Y_c are the two most important tracking scalars, which denotes the mixing between the fuel and the oxidizer and the progress of the combustion reaction from the reactants to products. In the present work, the progress variable is defined as follows.

$$Y_c = Y_{\mathrm{CO_2}} + Y_{\mathrm{CO}} + Y_{\mathrm{H_2O}} \tag{1}$$

The procedure of building up the FGM chemistry table is as follows. For each mixture fraction Z, a 1D premixed kerosene flame is computed using the open-source software CANTERA [7] together with the LUCHE skeletal mechanism [6]. The obtained chemical trajectory in 1D physical space is then remapped into the progress variable space. Specifically, for each value of the progress variable Y_c, the species mass fraction Y_i of the i-th species, the temperature and the also the source ω_{Yc} are obtained and stored into the chemistry table. It should be noted that linear interpolations are used when the mixture fraction is outside the flammability limit. Besides, additional chemical equilibrium trajectory is included for a better performance of describing the very slow chemical reactions towards the equilibrium at the fuel-rich side. Because fuel is injected into the combustor in liquid form, the temperature of the gas mixture must account for the energy required to evaporate the fuel. This is done by setting the enthalpy of the gaseous fuel equal to the enthalpy of the liquid kerosene [8].

To account for the subgrid turbulence-chemistry interaction, an additional tracking scalar of mixture fraction variance Z'' is employed in the FGM table. Presumed beta PDF distribution is used for describing the subgrid mixture fraction, and the FGM table is then convoluted with the beta PDFs at various levels of Z''. Due to the saturation of the kerosene evaporation, the maximum of the mixture fraction in the spray flame can never reach unity. The upper limit of the mixture fraction in the chemistry table is set to 0.4 here. The mixture fraction in the range of 0.0 to 0.4 is discretized over 201 points on a non-uniform grid. The grid is refined around ϕ = 1.0, where the species composition changes rapidly. The mixture fraction variance in the range of zero to its maximum, which equals to Z (1.0 – Z), is discretized on a non-uniform grid with 26 points. Finally, the progress variable in the range of 0.0 to its maximum, which is achieved at the equilibrium state, is discretized on a uniform

grid with 201 points. It should be noted that normalized quantities are employed as the FGM table coordinates for the three tracking scalars, and the normalized scalars are all in the range of zero to unity, which improves the accuracy of table look-up. Specially, the normalized progress variable is often denoted as C and it monotonically evolves from zero to unity for any single chemical trajectory. In summary, the FGM table features 201 × 26 × 201 data points for $Z \times Z'' \times C$. On each of these data points, the mass fractions of important species (such as fuel, O_2, H_2O and CO_2) and radicals (such as OH) and the source term ω_{Yc} are stored along with some important physical properties of the gas mixture, i.e., density, viscosity, diffusivity, heat capacity and molecular weight. The size of the complete FGM table is about 33 MB.

4. Large-eddy simulation

4.1 Gas phase modeling

The filtered Navier-Stokes (NS) equations in the low-Mach number form are solved for the gas phase [9]. The conservation equations for mass, momentum and three transported scalars are as follows:

$$\frac{\partial \overline{\rho}}{\partial t}+\frac{\partial \overline{\rho}\tilde{u}_j}{\partial x_j}=\overline{\dot{S}}_{m,d} \ , \tag{2}$$

$$\frac{\partial \overline{\rho}\tilde{u}_i}{\partial t}+\frac{\partial \overline{\rho}\tilde{u}_i\tilde{u}_j}{\partial x_j}=-\frac{\partial \overline{p}}{\partial x_i}+\frac{\partial}{\partial x_j}\left[\left(\overline{\mu}+\mu_T\right)\left(2\tilde{S}_{ij}-\frac{2}{3}\tilde{S}_{kk}\delta_{ij}\right)\right]+\overline{\dot{S}}_{mom,d,i} \ , \tag{3}$$

$$\frac{\partial \overline{\rho}\tilde{Z}}{\partial t}+\frac{\partial \overline{\rho}\tilde{u}_j\tilde{Z}}{\partial x_j}=\frac{\partial}{\partial x_j}\left(\overline{\rho}\left[F_D\Xi_\Delta\overline{D}+\left(1-\Omega\right)D_T\right]\frac{\partial \tilde{Z}}{\partial x_j}\right)+\overline{\dot{S}}_{m,d} \ , \tag{4}$$

$$\frac{\partial \overline{\rho}\tilde{Y}_c}{\partial t}+\frac{\partial \overline{\rho}\tilde{u}_j\tilde{Y}_c}{\partial x_j}=\frac{\partial}{\partial x_j}\left(\overline{\rho}\left[F_D\Xi_\Delta\overline{D}+\left(1-\Omega\right)D_T\right]\frac{\partial \tilde{Y}_c}{\partial x_j}\right)+\frac{\Xi_\Delta}{F_D}\overline{\dot{\omega}}_{Y_c} \ , \tag{5}$$

$$\begin{aligned}\frac{\partial \overline{\rho}\widetilde{Z^2}}{\partial t}+\frac{\partial \overline{\rho}\tilde{u}_j\widetilde{Z^2}}{\partial x_j}=&\frac{\partial}{\partial x_j}\left(\overline{\rho}\left[F_D\Xi_\Delta\overline{D}+\left(1-\Omega\right)D_T\right]\frac{\partial \widetilde{Z^2}}{\partial x_j}\right)\\&-2\overline{\rho}\overline{D}\left(\frac{\partial \tilde{Z}}{\partial x_j}\right)^2-\frac{2\overline{\rho}\overline{D}_T}{\Delta^2}\left[\widetilde{Z^2}-\left(\tilde{Z}\right)^2\right]+\overline{\dot{S}}_{Z^2,d}\end{aligned} \ , \tag{6}$$

where t is the time, ρ is density of the gas mixture, u is the gas velocity. The operator $\overline{\bullet}$ denotes spatial filtering while $\tilde{\bullet}$ denotes density-weighted spatial filtering. p is the pressure and S_{ij} is the strain rate. μ and D are the molecular viscosity and molecular mass diffusivity coefficient, respectively. μ_T and D_T are the turbulent eddy viscosity and turbulent mass diffusivity coefficient determined from the Germano dynamic procedure. The source terms due to the evaporation of droplet particles, $S_{m,d}$, $S_{mom,d,i}$, $S_{Z2,d}$, are computed using the particle-source-in-cell (PSI-CELL) model. From Eqs. (4) and (6), the subgrid scale (SGS) mixture fraction variance can be calculated as

$$Z''=\widetilde{Z^2}-\left(\tilde{Z}\right)^2 \ . \tag{7}$$

4.2 ATF combustion model

To make the partially premixed kerosene spray flame resolvable on the LES grid, the artificial thickened flame (ATF) model is applied. The broadening of the flame thickness is achieved by enhancing the molecular diffusivity by a thickening factor F_D and by dividing the source term of the progress variable by the same factor, as shown in Eqs. (4-6). The thickening factor F_D is dynamically computed as a function of the normalized progress variable to avoid unnecessary thickening of the preheat and burnout zones [10]:

$$F_D\left(C^*,Z\right)=\frac{\left(\mathrm{d}C/\mathrm{d}x\right)|_{C=C^*}}{\left(\mathrm{d}\overline{C}/\mathrm{d}x\right)|_{\overline{C}=C^*}} \ , \tag{8}$$

where the numerator $(\mathrm{d}C/\mathrm{d}x)|_{C=C^*}$ denotes the gradient of the C-profile, taken at $C = C^*$, obtained from the pre-computed 1D premixed flame at various levels of Z. The denominator $\left(\mathrm{d}\overline{C}/\mathrm{d}x\right)|_{\overline{C}=C^*}$ is

obtained through Gaussian-filtering, with a filter width Δ, of the same *C*-profile at $\overline{C} = C^*$. It has been demonstrated that the physics of the flame propagation can be well captured by such a dynamic thickening approach [10]. The filter width in LES simulation is set as $\Delta = \max\left(n\Delta_m, \delta_l^0\right)$, which ensures the reaction zone is resolved on a minimum of *n* grid points (*n* = 5 in the present work). The mesh cell size is denoted by Δ_m, while δ_l^0 is the laminar flame thickness which avoids unnecessary thickening when the flame is resolved on the mesh. Practically, the factor F_D is computed for various filter width and different values of *C** and *Z*, and tabulated prior to the LES simulation, to avoid performing on-the-fly Gaussian-filtering operations and therefore save the computational cost.

The flame sensor Ω is then calculated as $\Omega = (F_D - 1)/(\max(F_D) - 1)$, which takes a value of zero in fully burnt or unburnt regions and increases up to unity inside the flame. Inside the flame, the algebraic sub-filter wrinkling factor Charlette/Wang model is employed to compensate the loss of flame wrinkling due to the ATF approach:

$$\Xi_\Delta = \left(1 + \min\left[F - 1, \Gamma_\Delta\left(F, \frac{u'_\Delta}{s_l^0}, \mathrm{Re}_\Delta\right)\frac{u'_\Delta}{s_l^0}\right]\right)^\beta \quad . \tag{9}$$

F is the maximum thickening factor and is computed from:

$$F = \frac{\Delta}{\delta_l^0} \quad . \tag{10}$$

s_l^0 is the laminar flame speed and the sub-filter velocity fluctuation is estimated from:

$$u'_\Delta = 2\Delta_m^3 \left|\nabla^2\left(\nabla \times \tilde{\mathbf{u}}\right)\right|\left(\frac{n}{10}\right)^{1/3} = 2\Delta_m^3 \left|\nabla \times \left(\nabla^2 \tilde{\mathbf{u}}\right)\right|\left(\frac{n}{10}\right)^{1/3} \quad . \tag{11}$$

β = 0.5 is a model constant of Eq.(9).

4.3 Liquid phase modeling

The Lagrangian equations describing the transient position, velocity, temperature and mass of each droplet are written as:

$$\frac{\mathrm{d}x_{d,j}}{\mathrm{d}t} = u_{d,j} \quad , \tag{12}$$

$$\frac{\mathrm{d}u_{d,j}}{\mathrm{d}t} = \frac{f_1}{\tau_d}\left(\tilde{u}_j - u_{d,j}\right) + W_{sgs,j} \quad , \tag{13}$$

$$\frac{\mathrm{d}T_d}{\mathrm{d}t} = \frac{\mathrm{Nu}\, C_{p,g}\, f_2}{3\,\mathrm{Pr}\, C_{p,l}\, \tau_d}\left(T - T_d\right) + \frac{L_v}{m_d C_{p,l}}\frac{\mathrm{d}m_d}{\mathrm{d}t} \quad , \tag{14}$$

$$\frac{\mathrm{d}m_d}{\mathrm{d}t} = -\frac{\mathrm{Sh}\, m_d}{3\mathrm{Sc}\, \tau_d}\ln\left(1 + B_M\right) \quad , \tag{15}$$

where $x_{d,j}$ is the position of the droplet, $u_{d,j}$ is its velocity, T_d is its temperature and m_d is its mass.. Nu is the Nusselt number, Pr is the Prandtl number, Sh is the Sherwood number, Sc is the Schmidt number, and B_M is the Spalding number. The dynamic response time of a droplet is $\tau_d = \rho_l d^2 / \left(18\bar{\mu}\right)$, where ρ_l is its density, *d* is its diameter, $C_{p,l}$ is its heat capacity and L_v is the latent heat of vaporization. *T* and $C_{p,g}$ are the temperature and the heat capacity of the gas mixture, respectively. $W_{sgs,j}$ denotes the effects of unresolved SGS turbulence on particle acceleration, which is computed with a stochastic Markov model. f_1 is the drag factor accounting for high Reynolds number effects while f_2 is a correction factor for effects of heat exchange on droplet evaporation.

4.4 Numerical schemes and computational grid

The numerical scheme is based on an approach previously employed for both LES and DNS. The time advancement uses a second-order Crank-Nicolson scheme. A bound quadratic upstream

interpolation for convective kinematics (BQUICK) scheme is employed for advection terms of the scalar transport equations, while a second-order central difference scheme is applied to diffusion terms of the scalar transport equations and all terms of the momentum equation. An alternating direction implicit (ADI) approach is adopted, in which semi-implicit tridiagonal/pentadiagonal equations are solved separately for each direction.

The non-uniform computational grid used in the LES simulation is shown in Fig. 2. The minimum grid spacing is 700 μm at the edge of the swirling air nozzle, and the maximum on is 4.7 mm at the downstream exit of the domain. The number of grid cells is 2.26 M.

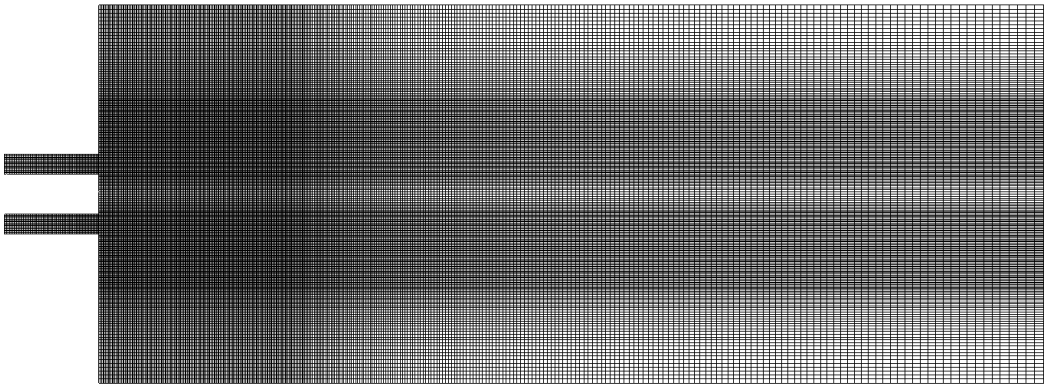

Figure 2 – Computational grid.

5. Results and discussions

5.1 Instantaneous two-phase flow fields

After injected into the combustor, a kerosene droplet is gradually heated up by the recirculated hot burnt gas and its mass decreases due to evaporation. Since the droplet density is assumed to be constant during the evaporation, the diameter of the droplet is decreasing with the release of gaseous kerosene fuel. An instantaneous snapshot of the swirling kerosene spray flame is shown in Fig. 3. The iso-surface of progress variable C = 0.5 is colored by the gas velocity. The iso-surface illustrates the actively burning flame area. It can be observed that the swirling kerosene spray is mainly burning at the upstream region of the combustor.

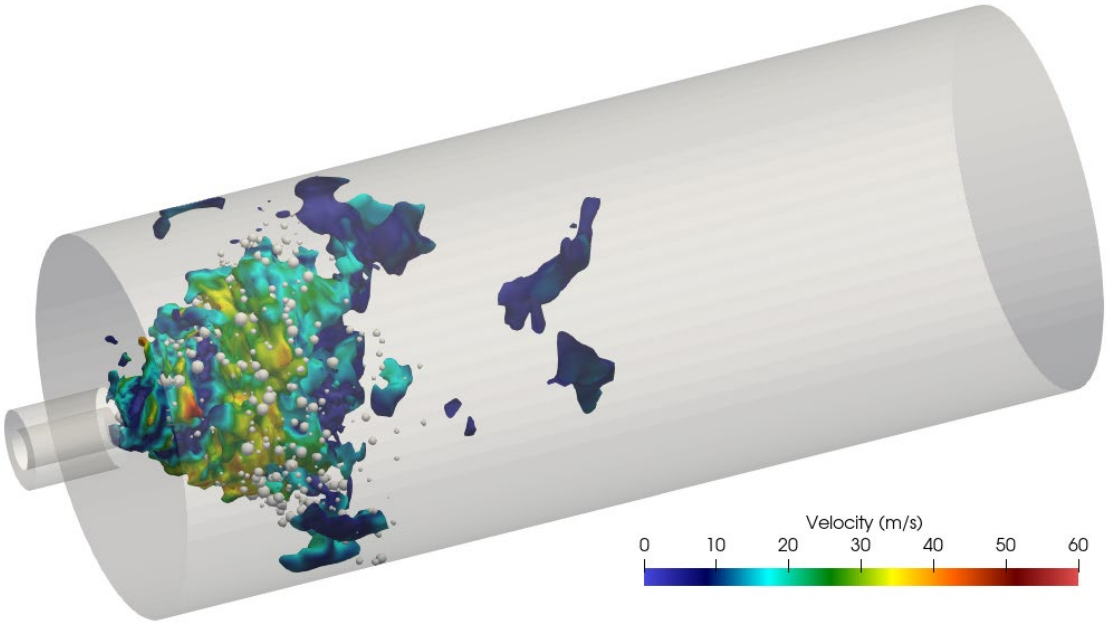

Figure 3 – Instantaneous kerosene droplet distribution and the C = 0.5 iso-surface, which is colored by gas velocity.

5.2 Transported scalar fields

The instantaneous contour fields of two transported scalar, i.e., mixture fraction and progress

variable, are shown in Figs 4 and 5, respectively. Because a high concentration of kerosene droplets near the fuel injection nozzle which are heated up by the recirculated hot gas, the evaporation source is quite large here and it features a high mixture fraction. From Fig. 5, it can be found that the flame propagates along the swirling cone. The motion of kerosene droplets is dominated by the swirling flow, especially for the smaller droplets with a low Stokes number. The high shear flow of the swirling air promotes the evaporation of kerosene droplets and enhances the turbulent mixing of evaporated fuel and air.

Figure 4 – Contours of instantaneous mixture fraction field.

Figure 5 – Contours of instantaneous progress variable field.

5.3 Comparison against experimental image

Figure 6 compares the temperature field predicted by the LES simulation against the experimental photo-image of the kerosene spray flame. It can be observed that the reaction zone featuring a conical shape is well predicted by the 3D LES simulation. It should be noted that the accurate prediction of the burning zone requires precise reproduction of the spatial location of the spray, as well as the droplet size and droplet temperature, which determines the local evaporation rate.

6. Conclusions

Large-eddy simulation of a swirl-stabilized kerosene spray flame is performed. The cylindrical combustion chamber is equipped with a cold swirling air stream. Liquid kerosene is injected from the fuel nozzle at the central recirculation zone. The two-phase turbulent flow features highly coupled phenomena, e.g., the evaporation of a fine spray in the presence of turbulent-chemistry interaction. The coupling of FGM chemistry table built with 3-component surrogate kerosene skeletal mechanism and the ATF model in the LES framework has been show capable of reproducing the partially premixed spray flame well. The present approach can be used for more complex turbulent spray flames of aeroengine combustors in the future.

7. Contact Author Email Address

* Corresponding author. Email address: cwjiang@buaa.edu.cn (C.W. Jiang)

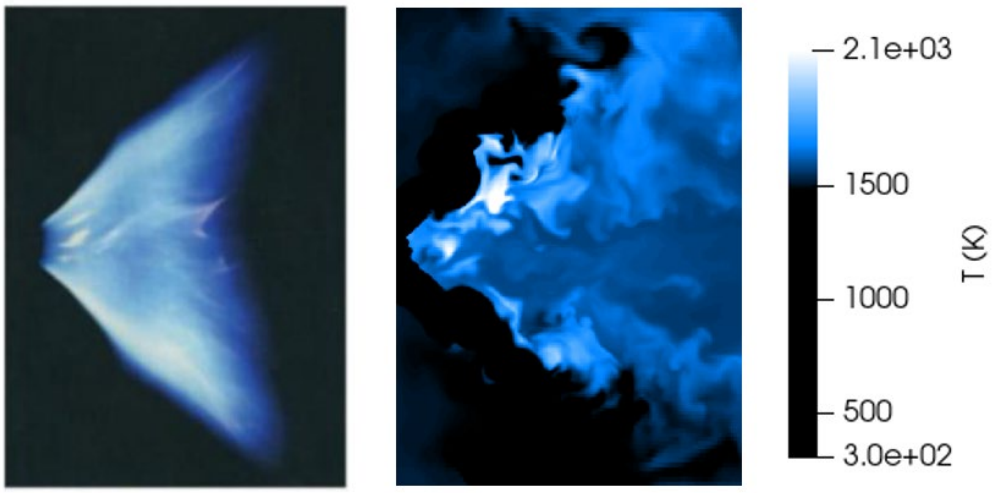

(a) Experimental photo (b) LES results

Figure 6 – Comparison between the experimental photo-image of the kerosene spray flame and the temperature field predicted by the LES simulation.

8. Acknowledgements

Financial support is kindly acknowledged from the National Natural Science Foundation of China (52076008, 11972061, 11872094, 11721202), the Zhejiang Provincial Natural Science Foundation (LGJ21E060001), the State Key Laboratory of Clean Energy Utilization (Open Fund Project No. ZJUCEU2020008).

9. Copyright Statement

References

[1] Moin, P. and Apte, S.V., Large-Eddy Simulation of Realistic Gas Turbine Combustors, *AIAA J.*, 44 (4), pp. 698-708, 2006.

[2] Honnet, S., Seshadri, K., Niemann, U. and Peters, N., A surrogate fuel for kerosene, *Proc. Combust. Inst.*, 32 (1), pp. 485-492, 2009.

[3] Nguyen, P.D., Vervisch, L., Subramanian, V. and Domingo, P., Multidimensional flamelet-generated manifolds for partially premixed combustion, *Combust. Flame*, 157 (1), pp. 43-61, 2010.

[4] Sheen, D.H. Swirl-stabilized spray flames in an axisymmetric model combustor. PhD Thesis, Imperial College, London, 1993.

[5] Domingo-Alvarez, P. High-pressure combustion large-eddy simulation for an a priori optical diagnostics validation. PhD Thesis, Normandie Université, 2019.

[6] Luche, J. Elaboration of reduced kinetic models of combustion. Application to a kerosene mechanism. PhD Thesis, Université d'Orléans, 2003.

[7] Goodwin, D.G., Moffat, H.K. and Speth, R.L. Cantera: An object-oriented software toolkit for chemical kinetics, thermodynamics, and transport processes. http://www.cantera.org

[8] Knudsen, E., Shashank and Pitsch, H., Modeling partially premixed combustion behavior in multiphase LES, *Combust. Flame*, 162 (1), pp. 159-180, 2015.

[9] Wan, K.D., Xia, J., Wang, Z.H., Pourkashanian, M. and Cen, K.F., Large-eddy Simulation of Pilot-assisted Pulverized-coal Combustion in a Weakly Turbulent Jet, *Flow Turbul. Combust.*, 99 (2), pp. 531-550, 2017.

[10] Proch, F., Domingo, P., Vervisch, L. and Kempf, A.M., Flame resolved simulation of a turbulent premixed bluff-body burner experiment. Part II: A-priori and a-posteriori investigation of sub-grid scale wrinkling closures in the context of artificially thickened flame modeling, *Combust. Flame*, 180, pp. 340-350, 2017.